Oncology Research, Vol. 27, pp. 713–727

0965-0407/19 $90.00 + .00
DOI: https://doi.org/10.3727/096504018X15433161908259
E-ISSN 1555-3906
www.cognizantcommunication.com

Extracellular S100A11 Plays a Critical Role in Spread of the Fibroblast Population in Pancreatic Cancers

Hitoshi Takamatsu,*[1] Ken-ichi Yamamoto,*[1] Nahoko Tomonobu,* Hitoshi Murata,* Yusuke Inoue,† Akira Yamauchi,‡ I Wayan Sumardika,*§ Youyi Chen,* Rie Kinoshita,* Masahiro Yamamura,¶ Hideyo Fujiwara,# Yosuke Mitsui,*,** Kota Araki,*†† Junichiro Futami,‡‡ Ken Saito,§§ Hidekazu Iioka,§§ I Made Winarsa Ruma,§ Endy Widya Putranto,¶¶ Masahiro Nishibori,## Eisaku Kondo,§§ Yasuhiko Yamamoto,*** Shinichi Toyooka,†† and Masakiyo Sakaguchi*

*Department of Cell Biology, Okayama University Graduate School of Medicine, Dentistry and Pharmaceutical Sciences, Okayama, Japan
†Faculty of Science and Technology, Division of Molecular Science, Gunma University, Kiryu, Gunma, Japan
‡Department of Biochemistry, Kawasaki Medical School, Kurashiki, Okayama, Japan
§Faculty of Medicine, Udayana University, Denpasar, Bali, Indonesia
¶Department of Clinical Oncology, Kawasaki Medical School, Kurashiki, Okayama, Japan
#Department of Pathology, Kawasaki Medical School, Kurashiki, Okayama, Japan
**Department of Urology, Okayama University Graduate School of Medicine, Dentistry and Pharmaceutical Sciences, Okayama, Japan
††Department of General Thoracic Surgery and Breast and Endocrinological Surgery, Okayama University Graduate School of Medicine, Dentistry and Pharmaceutical Sciences, Okayama, Japan
‡‡Department of Interdisciplinary Science and Engineering in Health Systems, Okayama University, Okayama, Japan
§§Division of Molecular and Cellular Pathology, Niigata University Graduate School of Medical and Dental Sciences, Niigata, Japan
¶¶Department of Pediatrics, Dr. Sardjito Hospital/Faculty of Medicine, Universitas Gadjah Mada, Yogyakarta, Indonesia
##Department of Pharmacology, Okayama University Graduate School of Medicine, Dentistry and Pharmaceutical Sciences, Okayama, Japan
***Department of Biochemistry and Molecular Vascular Biology, Kanazawa University Graduate School of Medical Sciences, Kanazawa, Ishikawa, Japan

The fertile stroma in pancreatic ductal adenocarcinomas (PDACs) has been suspected to greatly contribute to PDAC progression. Since the main cell constituents of the stroma are fibroblasts, there is crosstalking(s) between PDAC cells and surrounding fibroblasts in the stroma, which induces a fibroblast proliferation burst. We have reported that several malignant cancer cells including PDAC cells secrete a pronounced level of S100A11, which in turn stimulates proliferation of cancer cells via the receptor for advanced glycation end products (RAGE) in an autocrine manner. Owing to the $RAGE^{+}$ expression in fibroblasts, the extracellular abundant S100A11 will affect adjacent fibroblasts. In this study, we investigated the significance of the paracrine axis of S100A11–RAGE in fibroblasts for their proliferation activity. In in vitro settings, extracellular S100A11 induced upregulation of fibroblast proliferation. Our mechanistic studies revealed that the induction is through RAGE–MyD88–mTOR–p70 S6 kinase upon S100A11 stimulation. The paracrine effect on fibroblasts is linked mainly to triggering growth but not cellular motility. Thus, the identified pathway might become a potential therapeutic target to suppress PDAC progression through preventing PDAC-associated fibroblast proliferation.

Key words: S100A11; Pancreatic cancer; Fibroblasts; RAGE; Cancer microenvironment

[1]These authors provided equal contribution to this work.
Address correspondence to Masakiyo Sakaguchi, Ph.D., Department of Cell Biology, Okayama University Graduate School of Medicine, Dentistry and Pharmaceutical Sciences, 2-5-1 Shikata-cho, Kita-ku, Okayama-shi, Okayama 700-8558, Japan. Tel: +81-86-235-7395; Fax: +81-86-235-7400; E-mail: masa-s@md.okayama-u.ac.jp

INTRODUCTION

It has become evident that the tumor stroma has a critical role in the progression of various types of cancer. The tumor stroma is composed of multiple noncancerous cell populations, including fibroblasts, endothelial cells, and immune cells, and the extracellular matrix (ECM)[1–5]. Fibroblast cells appended to a mass of cancer cells, called cancer-associated fibroblasts (CAFs), are one of the major components of these cell populations (around 90% in the stroma)[2,6]. An enriched CAF population is frequently observed in pancreatic cancers, and it has been shown that CAFs accelerate pancreatic cancer progression toward malignancy concomitant with drug resistance, immunosuppression, and metastasis[1,5,6]. However, it is still not known how an increase in the CAF population occurs in pancreatic cancers. An understanding of the mechanism may be useful for the establishment of an effective antidote to CAFs.

S100A11, a small EF-hand-type calcium-binding protein with a molecular weight of about 10 kDa that belongs to the S100 family[7], has been reported to be overexpressed in pancreatic ductal adenocarcinomas (PDACs), and its overexpression is linked to poor survival[8]. We previously reported that S100A11 is secreted at significant levels from several kinds of cancer cells, especially epithelial cancer cells in the skin[9], mesothelioma cells[10,11], and pancreatic[10] cancer cells. The secreted S100A11 plays critical roles in acceleration of cellular proliferation, survival, and migration in an autocrine manner in cancer cells through a receptor for advanced glycation end products (RAGE)[7,9–12]. From these results, we had an idea that extracellular S100A11 secreted from cancer cells may function not only for the cells it is secreted from (autocrine) but also adjacent CAFs in a paracrine manner since fibroblasts also express RAGE. That may lead to a large CAF population in pancreatic cancer diseases. The significance of secreted S100A11 in CAFs has not been examined. Therefore, in this study, we aimed to clarify the extracellular role of S100A11 in proliferation of fibroblasts surrounding a tumor.

MATERIALS AND METHODS

Cell Lines

HEK293T cells (embryonic kidney cells stably expressing the SV40 large T antigen) and PK-8 cells (pancreatic carcinoma cells) were obtained from RIKEN BioResource Center (Tsukuba, Japan). A-431 cells (epidermoid carcinoma cells) and pancreatic cancer cell lines (PL45, AsPC-1, PANC-1, and BxPC-3) were obtained from ATCC (Rockville, MD, USA). Wild-type (WT) and RAGE$^{-/-}$ mouse embryonic fibroblasts (MEFs) were provided by Professor Yasuhiko Yamamoto (Kanazawa University, Kanazawa, Japan). MyD88$^{-/-}$ mouse fibroblasts were isolated from the resected lung of an MyD88$^{-/-}$ mouse (Oriental BioService, Kyoto, Japan). To stabilize the cell phenotype and avoid cellular senescence, the prepared primary mouse fibroblasts (WT, RAGE$^{-/-}$, and MyD88$^{-/-}$) were all immortalized in an autonomous manner through repeated passaging in cell culture. These human and mouse cells were all cultivated in D/F medium (Thermo Fisher Scientific, Waltham, MA, USA) supplemented with 10% FBS.

Recombinant Proteins

Highly purified human recombinant S100A11, S100A6, S100A8, S100A9, GST, and GST–MyD88 proteins were prepared as reported previously[9–13].

Reagents

To selectively inhibit intrinsic kinase activities of p70 S6 kinase and mTOR, we used p70 S6K inhibitor (PF-4708671; Cayman Chemical, Ann Arbor, MI, USA) and rapamycin (Merck, Kenilworth, NJ, USA), respectively. For a comparison study of kinases in activation states between WT and RAGE$^{-/-}$ fibroblasts, a human phospho-MAPK array kit (R&D Systems, Minneapolis, MN, USA) was used.

Protein Array

The detection procedure for the human phospho-MAPK array (R&D Systems) followed the manufacturer's instructions. After blocking the array membranes, the membranes were treated with prepared cell extracts (1.5 ml) for 2 h at RT and a series of the provided reagents (biotin-labeled anti-phospho antibodies and HRP-labeled streptavidin) one by one. Last, the washed membranes were all subjected to chemiluminescence detection equipped in the kit.

Expression Plasmids

MyD88 (WT)-HA gene expression constructs used in this study were made using the pIDT-SMART (C-TSC) vector[14] as the backbone to express the cargo gene, in which MyD88 was designed to be expressed as a C-terminal 3HA-6His-tagged form. Transient transfection of the above-described plasmids into cultured cells was performed using FuGENE-HD (Promega BioSciences, San Luis Obispo, CA, USA).

To obtain PK-8 clones that show a significantly high expression level of a foreign gene, either GFP alone or GFP+S100A11, in a stable manner, we succeeded in improving the pIDT-SMART (C-TSC) vector to a stable expression version, resulting in improved plasmids, named pSAKA-1B and pSAKA-4B. pSAKA-1B is highly adapted to Chinese hamster ovary (CHO) cells[15,16], whereas pSAKA-4B is adapted for a wide range of diverse cell lines of human origin in a constant and significantly

high expression manner. Using the improved plasmid pSAKA-4B, we established GFP- and GFP + S100A11-overexpressed clones from PK-8 cells through a convenient electroporation gene delivery method and following selection with puromycin at 20 mg/ml.

Western Blot Analysis

Western blot analysis was performed under conventional conditions. The antibodies used were as follows: a rabbit anti-human S100A11 antibody that we made[17–19], mouse anti-human S100A11 antibody (MBL, Nagoya, Japan), rabbit anti-S100A6 antibody (Cell Signaling Technology, Beverly, MA, USA), rabbit anti-calgranulin A (S100A8) antibody (Santa Cruz Biotechnology, Santa Cruz, CA, USA), rabbit anti-calgranulin B (S100A9) antibody (Santa Cruz Biotechnology), mouse anti-RAGE antibody (R&D Systems), mouse anti-tubulin antibody (Sigma-Aldrich, St. Louis, MO, USA), mouse anti-fibroblast antibody (EMD Millipore, Temecula, CA, USA), mouse anti- -smooth muscle actin antibody (DAKO Agilent Technologies, Santa Clara, CA, USA), rabbit anti-phospho-p70 S6 kinase antibody (Cell Signaling Technology), rabbit anti-p70 S6 kinase antibody (Cell Signaling Technology), rabbit anti-phospho-S6 antibody (Cell Signaling Technology), mouse anti-S6 antibody (Cell Signaling Technology), mouse anti-HA antibody (Cell Signaling Technology), and goat anti-GST antibody (GE Healthcare Bio-Sciences, Piscataway, NJ, USA).

Quantitative RT-PCR

Cultured cells were washed with phosphate-buffered saline, and total RNA was extracted using ISOGEN II Isolation Reagent (Nippon Gene, Tokyo, Japan). Then reverse transcription was performed using ReverTraAce qPCR RT Master Mix with gDNA Remover (TOYOBO, Osaka, Japan). Real-time PCR was performed using FastStart SYBR Green Master (Roche Applied Science, Penzberg, Upper Bavaria, Germany) with specific primers on a LightCycler 480 system II (Roche Applied Science): S100A11, forward primer: tctccaagacagagttc ctaagc; reverse primer: atcatgcggtcaaggacac; TBP (internal cont.), forward primer: gaacatcatggatcagaacaaca; reverse primer: atagggattccgggagtcat; Rps6kb1, forward primer: taaaggggctatggaaagg; reverse primer: ttaagcac cttcatggcaaa; Rps6kb2, forward primer: cctggagtgcct cagtgg; reverse primer: atggcccagggctagtgt; Tbp (internal cont.), forward primer: gggagaatcatggaccagaa; reverse primer: gatgggaattccaggagtca.

Immunohistochemistry

Human PDAC tissues were fixed in 10% buffered formalin solution. Paraffin-embedded sections were deparaffinized, and antigen retrieval was performed by microwave treatment. The sections were incubated with the first antibodies at 37°C for 1 h followed by the application of a second antibody, either Alexa594-conjugated goat anti-rabbit IgG antibody (Thermo Fisher Scientific) or Alexa488-conjugated goat anti-mouse IgG antibody (Thermo Fisher Scientific). The study using the tissue specimens was approved by the Research Ethics Committee in Kawasaki Medical School and Hospital (approved No. 3105). Informed consent was obtained from each patient for the use of these materials.

Cell Growth Assay

DNA synthesis was monitored by the incorporation of EdU into DNA. Cells were inoculated at a density of 2×10^5 cells per well into six-well plates and cultured in D/F medium with 10% FBS for 24 h and then starved with serum-free D/F medium for an additional 24 h. The starved cell cultures were treated with low-serum D/F medium (0.5% FBS) containing S100A11 (final concentration, 10 μg/ml) for 6 h, 12 h, and 24 h. EdU was added to the cultures 1 h before fixation of the cells, and the incorporated EdU was stained using a Click-iT™ EdU Alexa Fluor™ 594 Imaging Kit (Thermo Fisher Scientific) according to the manufacturer's instructions. CellTiter 96® AQueous One Solution Cell Proliferation Assay (MTS; Promega Biosciences) was used for assessment of cell proliferation. Cells were treated with S100A11 by the same method as that described above for DNA synthesis except for differences in the number of cells (1×10^4 cells) and culture plates (96-well plates).

Flow Cytometry

To track cell division, mouse fibroblasts (1×10^6 cells) were labeled with 10 μM Cell Trace Violet (CTV; Thermo Fisher Scientific) according to the manufacturer's instructions. PK-8 clones (1×10^5 cells) mixed with the same number of mouse fibroblasts (1×10^5 cells) were cocultured afterward. Flow cytometry was performed on a MACS Quant Analyzer (Miltenyi Biotec GmbH, Bergisch Gladbach, Germany) using MACS Quantify Software Ver. 2.5 (Miltenyi Biotec GmbH). Data were analyzed using FlowJo software (FlowJo; LLC; BD Biosciences, Franklin Lakes, NJ, USA).

Cell Migration Assay

Cell migration was assayed using a Boyden chamber method with filter inserts (pore size, 8 μm) in 24-well plates (BD Biosciences). Mouse fibroblasts (1×10^4 cells/insert) were seeded on the top chamber. The top chamber was filled with serum-free D/F medium, and the bottom chamber was filled with 0.5% FBS-low serum D/F medium. Recombinant S100A11 was then set in the bottom chamber at a final concentration of 0~10,000 ng/ml. After incubation

for 48 h, cells that appeared on the lower surface through the filter were counted after staining with hematoxylin and eosin (H&E) dye. The cell motility was then quantified by cell counting in five nonoverlapping fields at a magnification of 10× (objective lens) and was represented as the average of four independent experiments.

In Vitro Kinase Reaction

HEK293T cell extract was prepared by a lysis procedure of the cell pellets with a kinase buffer [50 mM Tris-HCl/pH 7.5, 150 mM NaCl, 5 mM $MgCl_2$, 1 mM DTT, PhosphoSTOP (Roche Applied Science), protease inhibitor cocktail (Roche Applied Science), and 1 mM ATP] including a detergent (0.5% Triton X-100). Purified GST or GST–My88 was then added to the extracts to a final concentration of 0~1 μg, and the mixtures were incubated at 25°C for 30 min.

In Vivo Tumor Model

PK-8 cells (2×10^6 cells or 3×10^6 cells) mixed with the same number of mouse fibroblasts (2×10^6 cells or 3×10^6 cells) were subcutaneously transplanted into BALB/c nu/nu mice (SLC, Hamamatsu, Japan). The size of tumors was measured with a vernier caliper, and tumor volume was calculated as $1/2 \times \text{shortest diameter}^2 \times \text{longest diameter}$.

Statistical Analysis

Data are expressed as means ± SD. We used simple pairwise comparison with Student's *t*-test (two-tailed distribution with two-sample equal variance). A value of $p < 0.05$ was considered significant.

RESULTS

PDAC Cells Actively Secrete S100A11

Figure 1 shows the typical features of PDAC tissue, which has a dense stroma surrounding the tumor (H&E staining). We confirmed the presence of an enriched fibroblast population in both the area surrounding the tumor and the intratumor area, suggesting an association between cancer cells and fibroblasts. The expression level of S100A11 was much higher in the tumor areas than in the fibroblasts (Fig. 1). Since the expression level of S100A11 was lower in fibroblasts, we next examined the expression levels of S100A11 in PDAC cell lines and fibroblast cell strains. Quantitative real-time PCR revealed that S100A11 has consistently high levels of expression in PDAC cell lines (PK-8, PL45, and AsPC-1) as well as in normal human OUMS-24 fibroblasts in comparison to its expression level in HEK293T cells (Fig. 2A). This expression pattern was the same as the pattern of protein expression in these cells except for PK-8 cells (Fig. 2B). However, interestingly, OUMS-24 fibroblasts, even cells with abundant S100A11, did not secrete S100A11, while PDAC cell lines showed active secretion of S100A11 (Fig. 2B). On the other hand, no obvious secretion of other PDAC-associated S100 proteins, S100A6, S100A8, and S100A9[20–22], was observed in the indicated PDAC cell lines (Fig. 2C). S100A8 and S100A9, which are highly expressed in inflammatory monocytes surrounding tumor stromas[23–25], were also not detected in PDAC cell extracts. Since the expression levels of RAGE, which functions as an S100A11 receptor, were almost the same in PDAC cells and fibroblasts (Fig. 2B),

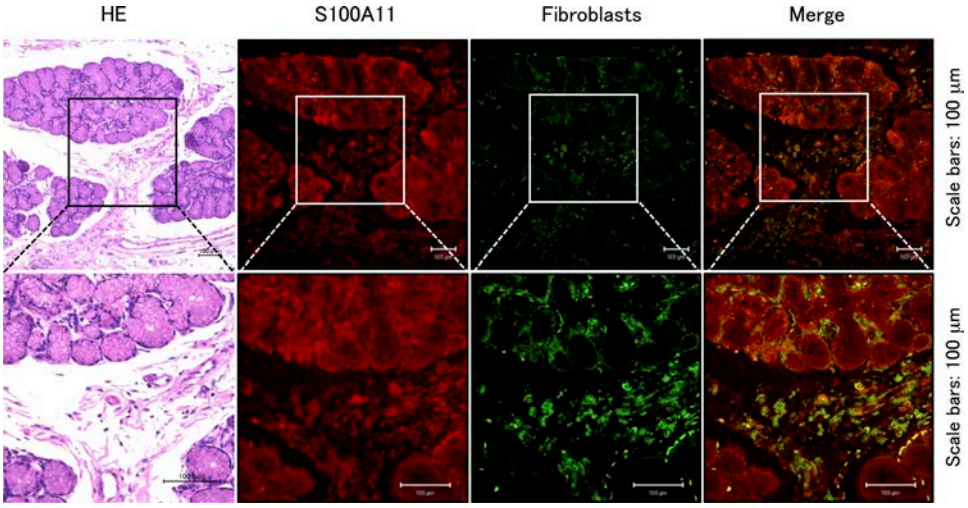

Figure 1. Expression state of S100A11 in pancreatic ductal adenocarcinomas (PDACs). Immunohistochemical analysis of S100A11 in PDAC tissue was performed. S100A11 and fibroblasts were immunostained in red and green colors, respectively. The pictures on the left show hematoxylin and eosin (H&E)-stained images corresponding to the immunofluorescence images on the right side. The results were confirmed by three similar experiments.

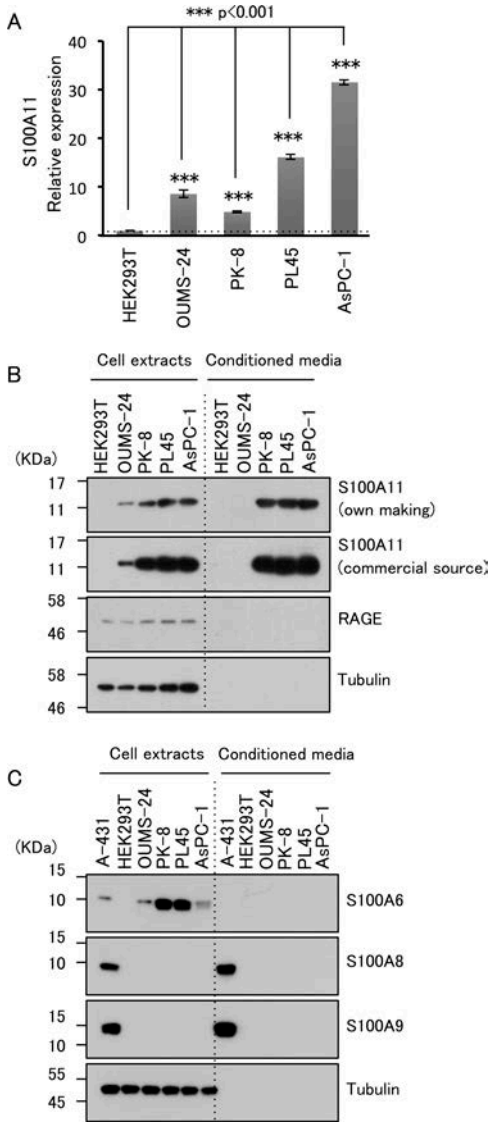

Figure 2. Expression and secretion states of S100A11 in PDAC cell lines. (A) Total RNAs prepared from various human PDAC cell lines (PK-8, PL45, and AsPC-1), normal human OUMS-24 fibroblasts, and SV40 large T antigen-expressed human embryonic kidney HEK293T cells were analyzed for expression of S100A11 by quantitative real-time PCR. TBP was used as a reliable internal control for calibration of the assessment. The results were confirmed by five similar experiments. (B, C) Protein specimens [cell extracts (left) and their corresponding conditioned culture media (right)] from the indicated cell lines were analyzed for S100A11 and receptor for advanced glycation end products (RAGE) (B) and S100A6, S100A8, and S100A9 (C) by Western blotting in a reduced condition. Tubulin was used as a control for loaded amounts of cell extracts and as a successful preparation of secreted proteins without any contamination of cellular proteins. The results were confirmed by an independent and two related experiments (B) or by three similar experiments (C).

PDAC-secreted extracellular S100A11 may function either in an autocrine manner for PDAC cells or in a paracrine manner for surrounding fibroblasts in vivo (Fig. 1).

Because the extracellular functions of S100A11 in CAFs have remained unclear in comparison to the autocrine role of S100A11 in cancer cells, we decided in this study to investigate the paracrine role of S100A11 in fibroblasts in a PDAC environment. We first tried to stimulate WT mouse fibroblasts with S100A11 recombinant proteins and found that extracellular S100A11 has the ability to upregulate proliferation of fibroblasts in a dose-dependent manner (Fig. 3A). In this assay, we found that 10 mg/ml (Fig. 3B) and 6 h (Fig. 3C) were the optimal concentration and time period to induce the highest activity for the stimulation of DNA synthesis. This condition was also applicable to other fibroblasts, mouse NIH/3T3 fibroblasts (Fig. 3D), and normal human OUMS-24 fibroblasts (data not shown). In addition, S100A11 showed the highest activity in growth stimulation of fibroblasts among the PDAC-associated S100 proteins under this experimental condition (Fig. 3E), and it did not show any positive contribution to the growth stimulation of PDAC cancer cells (PK-8, PANC-1, AsPC-1, and BxPC-3 cells) (Fig. 3F). Thus, we hypothesized that PDAC cell-secreted S100A11 acts as a trigger to stimulate the proliferation of CAFs via RAGE, which may play a critical role in triggering a stroma-enriched PDAC phenotype (Fig. 3G).

The S100A11–RAGE Axis in Fibroblasts Plays an Important Role in PDAC Growth Through Upregulation of Fibroblast Growth

To investigate the role of the S100A11–RAGE axis in fibroblasts in the progression of PDACs with a dense stroma in vivo, wild-type mouse fibroblasts (WT fibroblasts) or RAGE KO mouse fibroblasts ($RAGE^{-/-}$ fibroblasts) were mixed with PK-8 cells, which show high levels of expression and secretion of S100A11 at the protein level (Fig. 2B), at a rate of 1:1 and transplanted subcutaneously into the backs of mice (Fig. 4A). This in vivo experiment also included single transplantations of PK-8 cells, WT fibroblasts, and $RAGE^{-/-}$ fibroblasts. At first, we confirmed that no sign appeared from the injected fibroblasts (WT and $RAGE^{-/-}$) for its derived tumorigenesis (Fig. 4B and C). Tumor growth with single transplantation of PK-8 cells was very slow; however, the tumors derived from PK-8 cells showed a highly aggressive phenotype in growth when the PK-8 cells were combined with WT fibroblasts (Fig. 4B and C). The results spurred us to examine the role of RAGE in fibroblasts in PDAC growth in vivo. By a similar approach, we surprisingly found a pronounced difference in tumor growth throughout the observation period (i.e., the rate of growth was much lower in the case of $RAGE^{-/-}$ fibroblasts than in the

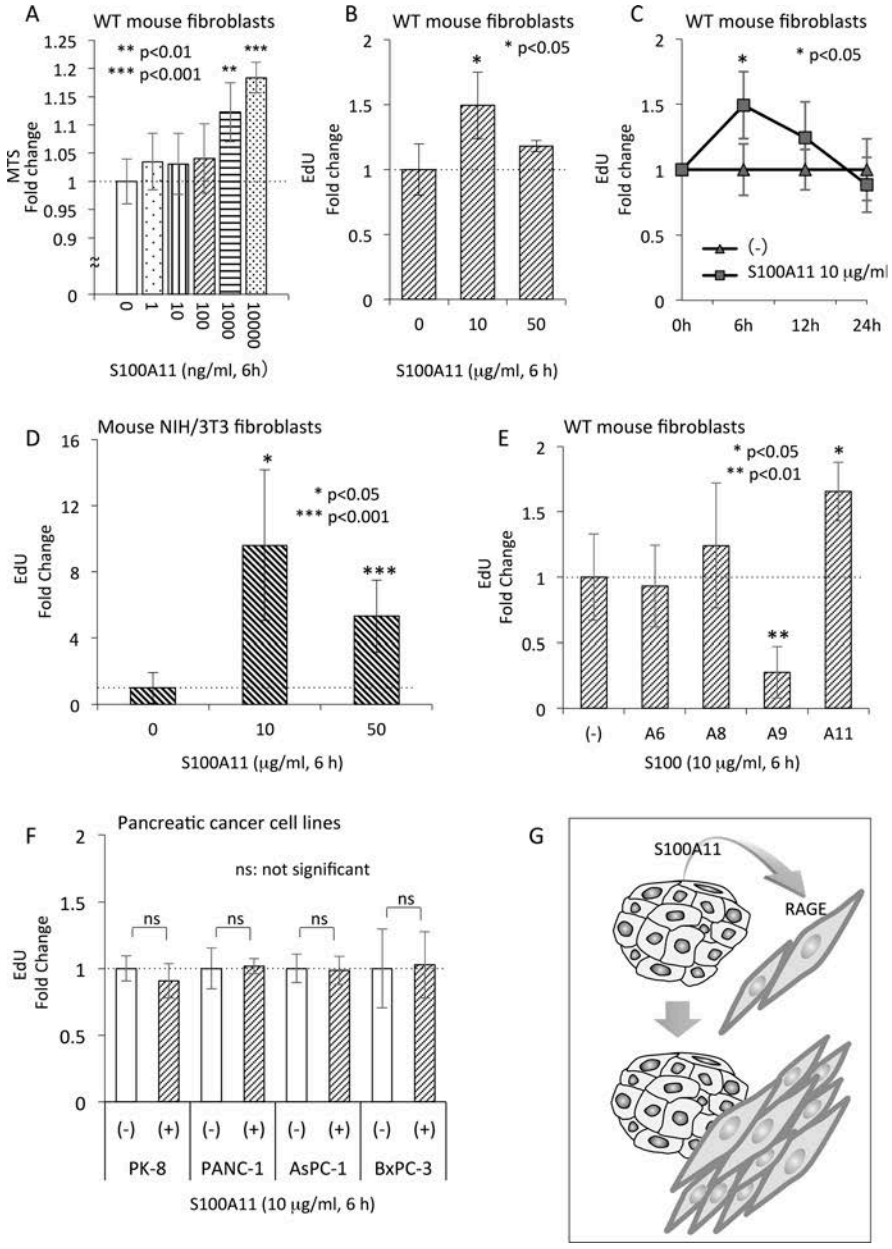

Figure 3. S100A11-mediated upregulation of the growth of fibroblasts. (A) MTS and (B) EdU uptake assays were performed for wild-type (WT) mouse fibroblasts after stimulation of the cells with increased doses of recombinant S100A11 for 6 h. The results were confirmed by five similar experiments (A) or by an independent and four related experiments (B). (C) Time-dependent EdU uptake was evaluated in WT mouse fibroblasts after stimulation of the cells with S100A11 at a final concentration of 10 mg/ml. The results were confirmed by three similar experiments. (D) An EdU uptake assay was performed for mouse NIH/3T3 fibroblasts by the same method as that described in (B). The results were confirmed by an independent and three related experiments. (E) Growth stimulation ability of each S100 protein (S100A6, S100A8, S100A9, and S100A11) was evaluated in WT mouse fibroblasts by the same EdU uptake assay. All of the S100 proteins were used at a final concentration of 10 mg/ml for 6 h. The results were confirmed by another two similar experiments. (F) EdU uptake assays were also performed for the indicated PDAC cells (PK-8, PANC-1, AsPC-1, and BxPC-3 cells) after stimulation of each cell line with S100A11 at a final concentration of 10 mg/ml for 6 h. The results were confirmed by an independent and three related experiments. (G) Schematic of the hypothesis of PDAC-secreted S100A11 inducing a proliferation burst of surrounding fibroblasts via cell surface RAGE.

case of WT fibroblasts when combined with PK-8 cells) (Fig. 4D). This was also obvious on the last experimental day (day 20) for assessment of tumor weights (Fig. 4E). The tumor weights were reduced in the RAGE$^{-/-}$ group. In addition, immunohistochemistry of resected tumor tissues showed a markedly smaller fibroblast population in the RAGE$^{-/-}$ fibroblast mixed tumors than in the tumors with a combination of WT fibroblasts (Fig. 4F).

Because of the multiple ligands other than S100A11 that RAGE has in in vivo environments[17], we next examined

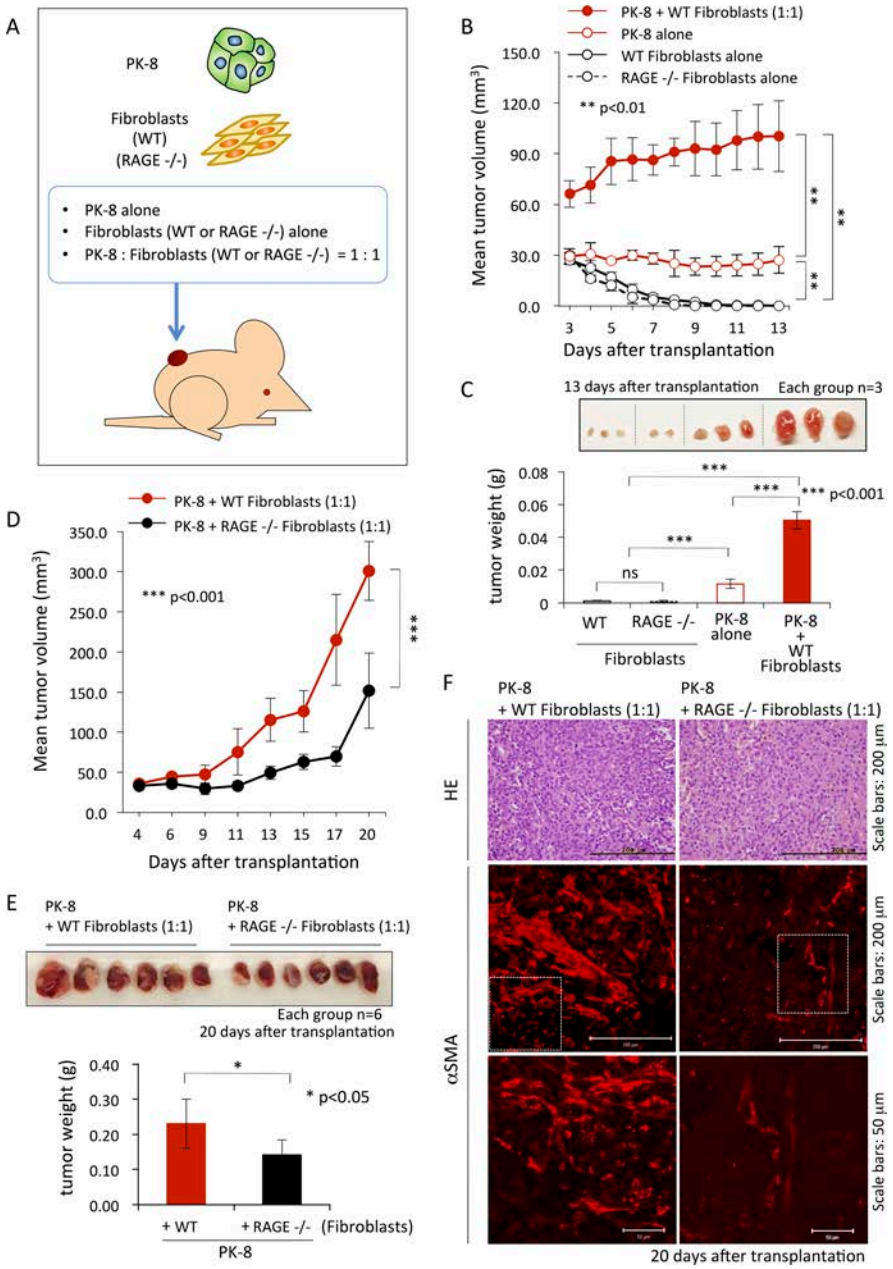

Figure 4. Effect of RAGE knockout in fibroblasts on PDAC progression in vivo. (A) Schematic of subcutaneous single transplantation of PK-8 cells and mouse fibroblasts (WT or RAGE$^{-/-}$) and cotransplantation of PK-8 cells with either WT or RAGE$^{-/-}$ mouse fibroblasts in a cell number ratio of 1:1 in the back of a nude mouse (BALB/c nu/nu). (B and D) Tumor sizes were monitored on the indicated days after transplantation of the prepared cells. (B) PK-8 cells alone (2×10^6 cells), mouse fibroblasts (WT or RAGE$^{-/-}$) alone (2×10^6 cells), PK-8 cells (2×10^6 cells)+WT mouse fibroblasts (2×10^6 cells). (D) PK-8 cells (3×10^6 cells)+mouse fibroblasts (WT or RAGE$^{-/-}$) (3×10^6 cells). Tumor weights were quantified 13 days (C) and 20 days (E) after transplantation. (F) Histology of tumors as shown in (E) was examined. H&E, hematoxylin and eosin staining. Anti- -smooth muscle actin (SMA) antibody was used for identification of fibroblasts in the tumors that had formed. Scale bars in H&E-stained panels: 200 μm; scale bars in immunofluorescence-stained panels: 200 μm (top) and 50 μm (bottom). These results (B–F) were confirmed by two independent and three related experiments.

the significance of the S100A11–RAGE axis in the proliferation of fibroblasts in a coculture system consisting of mouse fibroblasts (WT and RAGE$^{-/-}$ fibroblasts) and PK-8 sublines that stably overexpressed control GFP alone (GFP) and both GFP and S100A11 (GFP + S100A11) in different combinations. To examine accurately the growth activity of fibroblasts in this culture system, we labeled fibroblasts with the dye Cell Trace Violet (CTV) before coculture and monitored their division states at regular time intervals by flow cytometry (Fig. 5A). There is an inverse relation between cell division number and CTV fluorescence intensity in this assay. The labeled fibroblasts and PK-8 clones were separated according to the fluorescence differences between CTV and GFP, respectively (Fig. 5B), and we found that the division of mixed fibroblasts (WT fibroblasts) was actually upregulated by

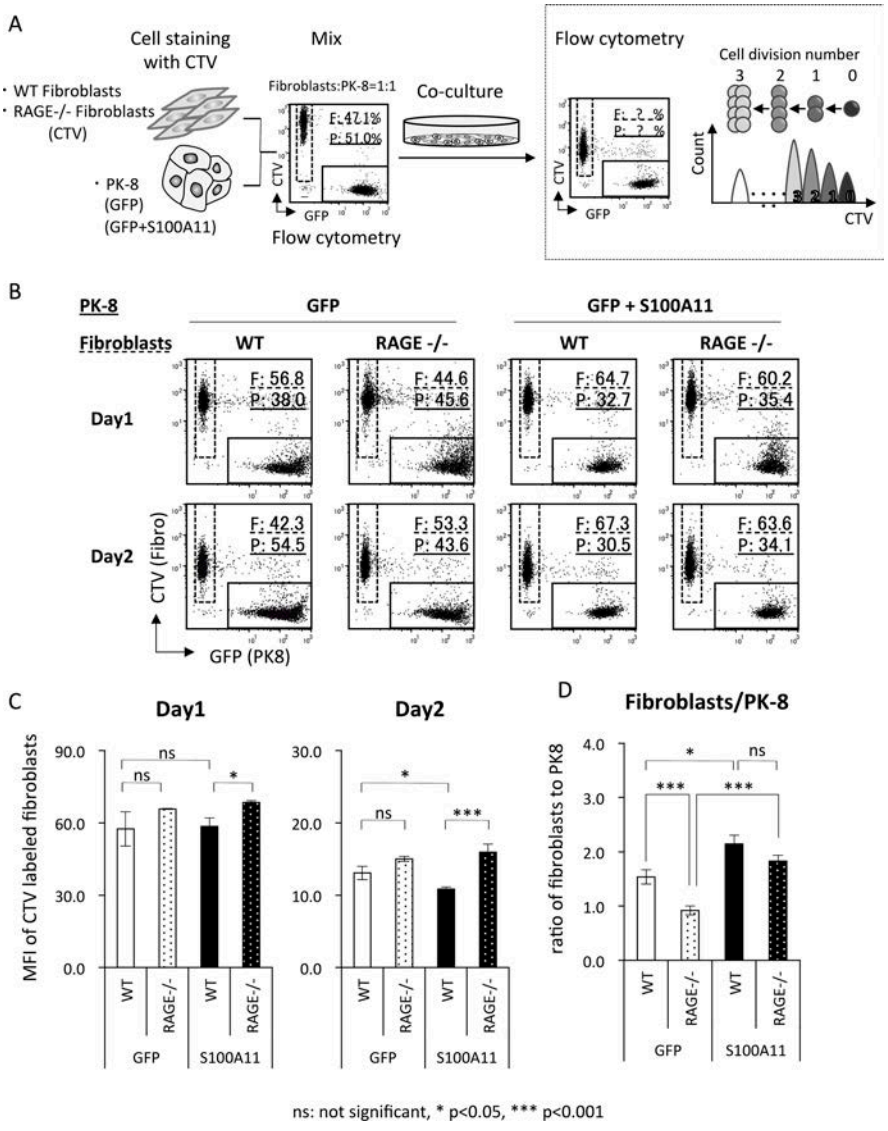

Figure 5. Effect of the S100A11–RAGE axis on division of fibroblasts in a coculture system with PK-8 cells. (A) Schematic flow of the evaluation. PK-8 clones that stably overexpressed GFP or GFP + S100A11 were cocultured with either CTV-labeled WT or RAGE$^{-/-}$ mouse fibroblasts in a cell number ratio of 1:1 with different combinations. After cultivation of the mixed culture, PK-8 cells and fibroblasts were separated according to the different fluorescence colors (GFP: *x*-axis, CTV: *y*-axis) and evaluated for division states of the fibroblasts (CTV) by flow cytometry. (B) The mixed cells were cultured for 1 day (day 1) and 2 days (day 2). The labeled cells were detected by flow cytometry. The enclosed squares with dotted line represent CTV-labeled fibroblasts (F), while the squares with simple line show GFP-labeled PK-8 cells (P). The gated cell populations (F and P) were displayed as % at the upper right corners. (C) The graphs are quantified results from (B). MFI represents each value of fluorescence intensity from the gated fibroblast population (F). (D) Ratios of the cell populations included in the cocultures at 1 day were finally quantified and expressed as values of CTV-labeled fibroblasts (F, %)/GFP-labeled PK-8 cells (P, %). The experiment was performed in triplicate and the results were also confirmed by two related experiments.

the combination with S100A11-overexpressed PK-8 cells in comparison to the combination with control GFP cells at day 2 (Fig. 5C). In addition, the division was markedly impaired in the case of using RAGE$^{-/-}$ fibroblasts. To express these events more clearly, we finally calculated the ratios of fibroblasts to PK-8 cells in the cocultures. We found that the number of fibroblasts was the largest in the coculture with S100A11-overexpressed PK-8 cells and fibroblasts (WT fibroblasts) and showed a tendency to be reduced in the case of the combination with KO fibroblasts (RAGE$^{-/-}$ fibroblasts). This implies that there is a positive role of the S100A11–RAGE axis in the proliferation of fibroblasts (Fig. 5D). The S100A11–RAGE axis in fibroblasts may also positively affect the growth of adjacent PDAC cells because we found that the division ratio of PK-8 cells was markedly higher in the case of coculture with WT fibroblasts than that with RAGE$^{-/-}$ fibroblasts (Supplementary Fig. 1, available at: https://www.dropbox.com/sh/pl31smto8gq5v8v/AAAFle3bURFnT8-eRhh4V6FJa?dl=0). Collectively, these results suggest an unusual role of the S100A11–RAGE axis in the growth of PDAC-associated fibroblasts that is linked to PDAC progression in part through fertilization of the surrounding stroma and its enforced direct stimulation of the proliferation of PDAC cells.

S100A11–RAGE Binding Induces Sustained Activation of p70 S6 Kinase via MyD88 in Fibroblasts

We tried to determine how the proliferation of PDAC-associated fibroblasts is regulated by RAGE upon S100A11 binding by first utilizing an activated kinases screening array. The results interestingly showed an increase in phosphorylation of p70 S6 kinase in mouse fibroblasts (WT fibroblasts) but not in RAGE$^{-/-}$ fibroblasts (Fig. 6A). The fact that p70 S6 kinase plays a crucial role in cellular proliferation was also a reason for our interest in the results. We previously reported that TIRAP and MyD88 proteins act as critical adaptors to RAGE and that they are able to interact with the RAGE cytoplasmic tail and function in the regulation of diverse downstream signal pathways of RAGE upon ligand binding[12,23,26]. We hence explored the possible linkage between p70 S6 kinase and MyD88. Three kinds of mouse fibroblasts (WT, RAGE$^{-/-}$, and MyD88$^{-/-}$ fibroblasts) were prepared. The fibroblasts were stimulated with S100A11, and the activation level of p70 S6 kinase in each cell specimen was evaluated. We observed pronounced induction of the phosphorylation of p70 S6 kinase with the highest activity at 3 h and sustained activation up to 24 h in WT fibroblasts (Fig. 6B). On the other hand, RAGE$^{-/-}$ cells showed induction of p70 S6 kinase phosphorylation at 3 h but no sustained activation. Interestingly, no induction occurred during S100A11 treatment in MyD88$^{-/-}$ cells. In this experiment, we confirmed that there was no appreciable difference in the expression of mouse genes producing p70 S6 kinase, Rps6kb1, and Rps6kb2, between WT and RAGE$^{-/-}$ fibroblasts even after stimulation with S100A11 (Fig. 6C). To confirm the essential role of MyD88 in the S100A11–RAGE-mediated activation of p70 S6 kinase in fibroblasts, we performed forced expression of foreign MyD88 in MyD88$^{-/-}$ cells. As a result, the phosphorylation of p70 S6 kinase in response to S100A11 was recovered in the transduced MyD88$^{-/-}$ cells (Fig. 6D). These results indicate an essential role of MyD88 in the process of activation of p70 S6 kinase through S100A11–RAGE signaling in fibroblasts.

MyD88 Greatly Contributes to Triggering the Activation Cascade of mTOR–p70 S6 Kinase That Induces Fibroblast Proliferation

In order to reinforce the strong association between MyD88 and p70 S6 kinase, we used an in vitro kinase reaction system based on a nondenatured cell extract that was supplemented with or not supplemented with purified recombinant proteins (control GST or GST–MyD88) and adenosine triphosphate (ATP) (Fig. 7A). In this assay, we found that phosphorylation of endogenous S6 ribosome, which is mainly phosphorylated by S6 kinases, was dramatically elevated by the inclusion of GST–MyD88 in a dose-dependent manner (Fig. 7B). This did not occur in either the condition of control GST addition or the condition of no addition. Furthermore, the GST–MyD88-mediated phosphorylation of S6 ribosome was efficiently reduced by the presence of either a selective inhibitor of p70 S6 kinase (p70S6K inhibitor) or the mTOR inhibitor rapamycin (Fig. 7C), indicating the certain presence of mTOR molecules in the MyD88–p70 S6 kinase signal flow.

We last tried to confirm the importance of the identified pathway triggered by S100A11–RAGE binding in growth stimulation of fibroblasts. As shown in Figure 8A, although WT fibroblasts showed a strong response to S100A11, which caused increased DNA synthesis, RAGE–KO fibroblasts showed no positive reaction to S100A11. In the case of MyD88$^{-/-}$ cells, S100A11 stimulation resulted in abolishment of DNA synthesis. In addition, S100A11-induced upregulation of growth was markedly suppressed by treatment of the fibroblasts with either the selective inhibitor of p70 S6 kinase or rapamycin (Fig. 8B). We hence emphasize an unusual role of the MyD88-mediated signal flow to link an activation of mTOR–p70 S6 kinase that is linked to an increase in fibroblast proliferation, which may eventually contribute to the fertile stroma associated with PDACs (Fig. 8C).

DISCUSSION

A fertile stroma, which frequently appears in PDACs, is an issue that must be solved for PDAC treatment

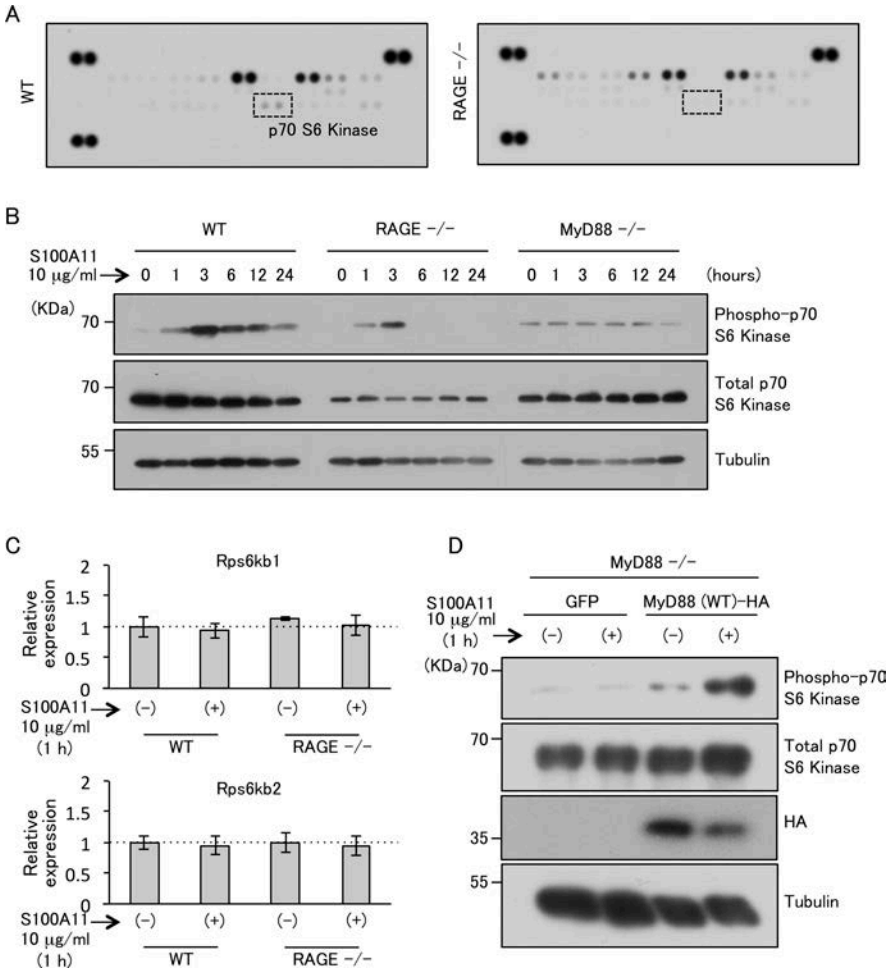

Figure 6. Activation of p70 S6 kinase through the S100A11–RAGE–MyD88 axis in fibroblasts. (A) Kinases at different activation levels were analyzed using an antibody array for WT mouse fibroblasts in comparison to RAGE$^{-/-}$ mouse fibroblasts. A dotted square indicates the antibody against phospho-p70 S6 kinase. The array screening was done by one experiment. (B) The phosphorylation status of p70 S6 kinase was monitored at regular time intervals for 24 h in WT, RAGE$^{-/-}$ and MyD88$^{-/-}$ mouse fibroblasts. The results were confirmed by five similar experiments. (C) Total RNAs prepared from the indicated cells treated or not treated with S100A11 were analyzed for the expression of Rps6kb1 and Rps6kb2 by quantitative real-time PCR. Tbp was used as a reliable internal control for calibration of the assessment. The results were confirmed by three similar experiments. (D) Western blot analysis of phospho-p70 S6 kinase was done for MyD88$^{-/-}$ mouse fibroblasts after transfection with either GFP or MyD88 (WT)-HA tag in the presence or absence of extracellular S100A11. The results were confirmed by five similar experiments.

because the stroma acts to prevent efficient delivery of drugs to the cancer site and to cause a metastatic phenotype of cancer cells[1–6]. However, due to an insufficient understanding of the mechanistic events that include crosstalking with multiple cell types in a cancer environment that requires a large number of multiple molecules, treatment is very difficult. In this study, we focused on the mechanism of accelerated proliferation of fibroblasts in the PDAC stroma since fibroblasts were shown to occupy most of the PDAC stroma area (around 90%)[2,6]. Growth of stroma fibroblasts may be positively affected by adjacent PDAC cells through PDAC-derived soluble factors, eventually leading to stroma enrichment in PDAC. We previously reported that S100A11 is actively secreted from squamous cell carcinoma, mesothelioma and PDAC cells and that the secreted S100A11 stimulates cancer cells to upregulate proliferation of cancer cells in an autocrine manner by way of the RAGE receptor[7,9–11]. However, the functions of secreted S100A11 from cancer cells in the surrounding stroma, especially in fibroblasts, have not been clarified. Owing to the RAGE^{+} expression in fibroblasts, S100A11 will stimulate fibroblasts (Fig. 2B). Our study revealed for the first time that PDAC-secreted S100A11 is able to induce an increase in the growth of surrounding fibroblasts through the TIRAP/MyD88–mTOR–p70S6K cascade (Fig. 8C), which may greatly contribute to fertilization of the stroma in PDAC. The linkage

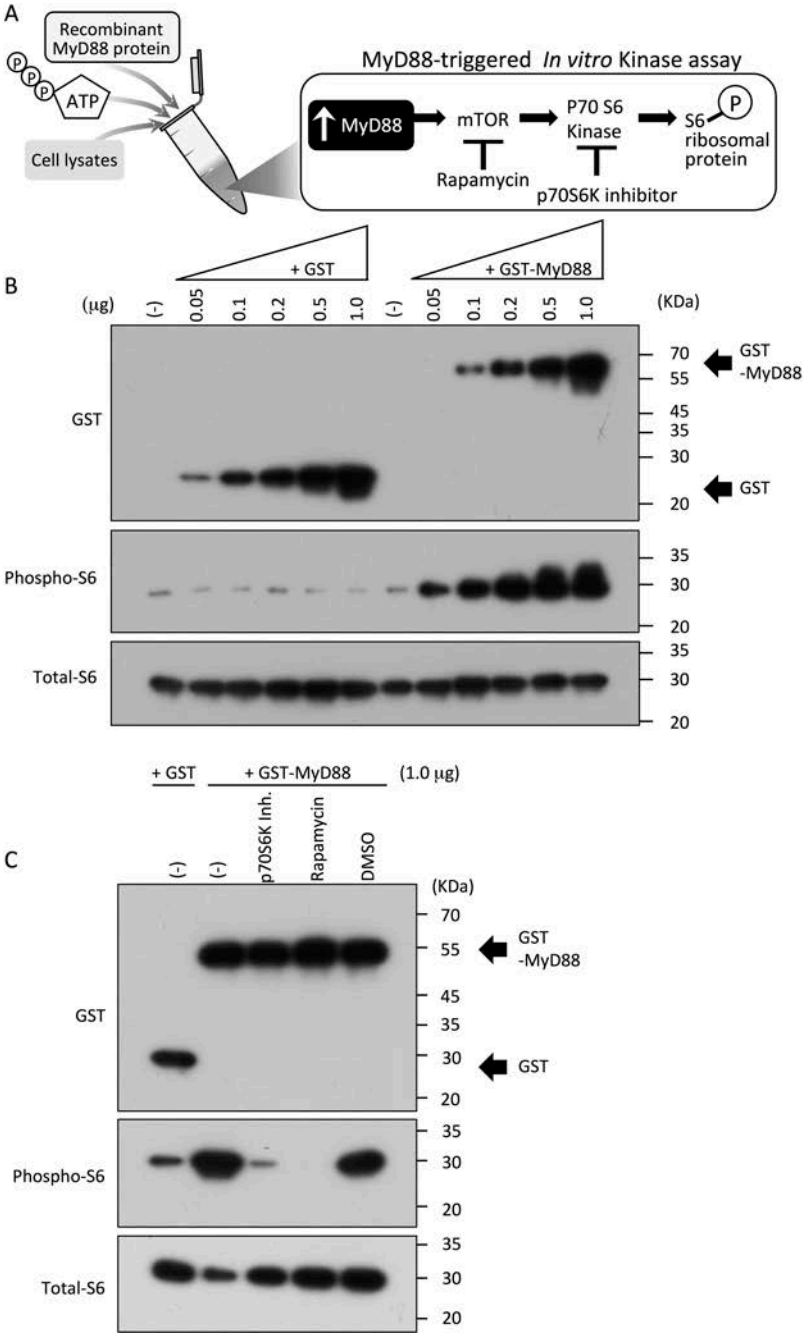

Figure 7. Critical role of MyD88 in activation of the mTOR–p70 S6 kinase cascade. (A) Schematic of the MyD88-triggered in vitro kinase reaction. (B) Cell extracts were prepared from HEK293T cells under a nondenatured condition. The cell extracts were supplemented with ATP (final concentration, 1 mM) and treated with either GST or GST–MyD88 recombinant protein in a range of final concentrations of 0~1.0 mg for 30 min. The reactants were analyzed for phosphorylation of S6 ribosome from HEK293T cells by Western blotting. The results were confirmed by three similar experiments. (C) The same experiment as that described in (B) was performed except for the use of selective inhibitors of p70 S6 kinase (p70S6K inhibitor; final concentration, 1 nM) and mTOR (rapamycin; final concentration, 5 nM) (A). The results were confirmed by three similar experiments.

of TIRAP/MyD88 and mTOR is reasonable because MyD88 can recruit PI3K[27], which in turn phosphorylates AKT, resulting in activation of mTOR. A linkage between MyD88 and mTOR has also been shown in a study on the TLR9 downstream pathway[28]. In addition, Chang et al. demonstrated an essential role of MyD88 in sustained activation of mTOR that leads to accelerated proliferation of T-helper 17 (Th17) cells[29].

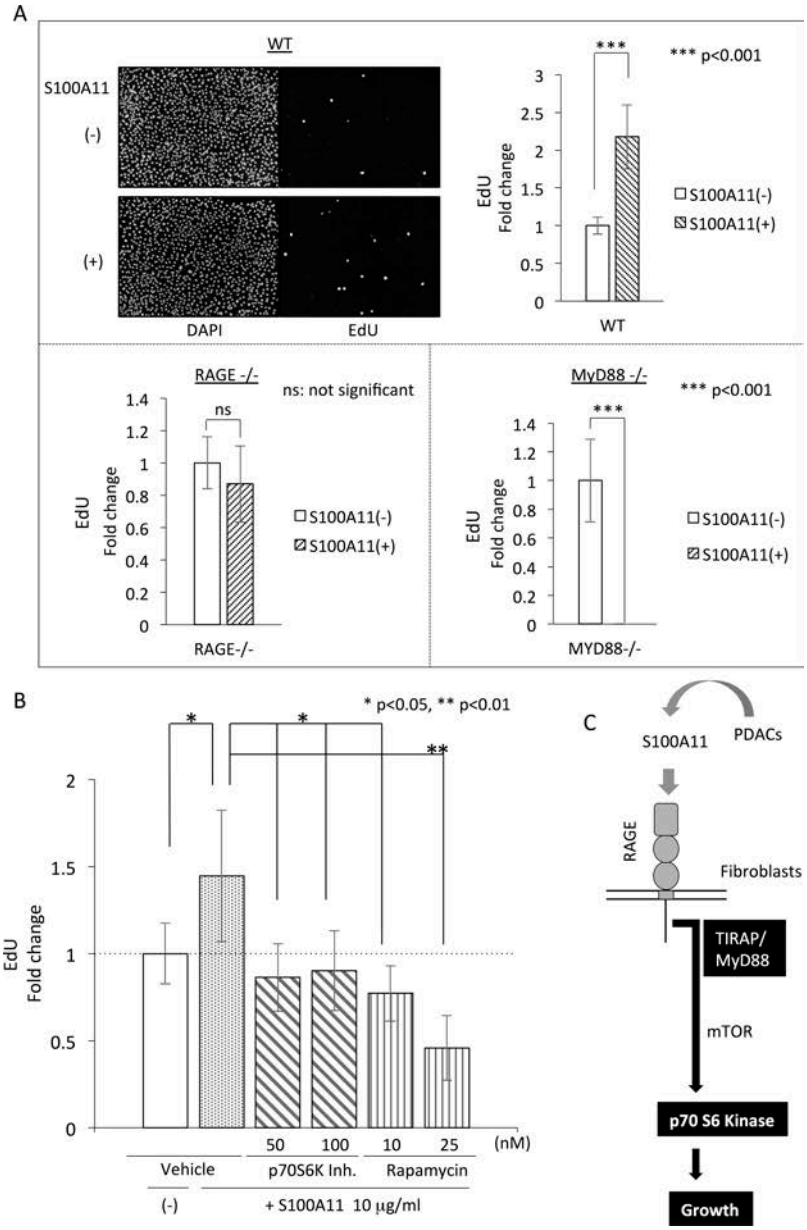

Figure 8. Critical role of the identified pathway (S100A11–RAGE–mTOR–p70 S6 kinase) in induction of fibroblast growth. (A) EdU staining was performed in the indicated cells, WT, RAGE$^{-/-}$ and MyD88$^{-/-}$ mouse fibroblasts that were treated or not treated with 10 mg/ml (final concentration) of S100A11 for 6 h. The results were confirmed by three related experiments. (B) EdU staining was also performed in S100A11-stimulated WT mouse fibroblasts that were pretreated with either p70S6K inhibitor or rapamycin. The results were confirmed by five similar experiments. (C) Model of the S100A11–RAGE-mediated proliferation pathway in PDAC-associated fibroblasts.

RAGE plays a crucial role in not only growth but also cellular motility (Supplementary Fig. 2A, available at: https://www.dropbox.com/sh/pl31smto8gq5v8v/AAAFle3bURFnT8-eRhh4V6FJa?dl=0). To study the role of S100A11–RAGE–MyD88 in migration of fibroblasts, we used MyD88$^{-/-}$ cells as well as RAGE$^{-/-}$ cells. Complete abrogation of RAGE and MyD88 genes resulted in marked reduction of S100A11-mediated stimulation of the growth of fibroblasts (Fig. 8A). Interestingly, migration of WT fibroblasts was not induced by S100A11 stimulation. On the other hand, the basal migration level was significantly downregulated in RAGE$^{-/-}$ cells even with S100A11 stimulation (Supplementary Fig. 2B, left). In contrast, MyD88$^{-/-}$ cells showed highly elevated activity for basal cellular motility. In addition to TIRAP/MyD88, RAGE has other adaptor molecules, including mDia-1[30]

and DOCK7[31], that dominantly contribute to the activation of cellular migration (Supplementary Fig. 2A), and they may therefore be in an overactivated state because of the loss of the MyD88 pathway, resulting in a pronounced increase in migration activity (Supplementary Fig. 2B, right). We hence speculate that there are S100A11-dependent and independent pathways in RAGE: MyD88 functions in the former pathway, and mDia-1 and DOCK7 contribute to the latter pathway.

As shown in Figure 5D, despite the increased division of the fibroblast population (WT fibroblasts) in the coculture with S100A11-overexpressed PK-8 cells in comparison to that in the coculture with control PK-8 cells (GFP), the elevation was not significantly reduced in RAGE$^{-/-}$ fibroblasts. This may be due to the activation of p70 S6 kinase in RAGE$^{-/-}$ fibroblasts at an early phase after stimulation with S100A11 (Fig. 6B). These points may be explained by the presence of receptors similar to RAGE that may react with exogenous S100A11. In that respect, we have reported RAGE-like receptors, such as melanoma cell adhesion molecule (MCAM), activated leukocyte cell adhesion molecule (ALCAM), extracellular matrix metalloproteinase inducer (EMMPRIN), neuroplastin (NPTN), and embigin (EMB), that react with other S100 family proteins including S100A8/A9, a heterodimer complex composed of S100A8 and S100A9, and S100A4[32–35]. We investigated the expression levels of those receptors in RAGE$^{-/-}$ fibroblasts using the RNA-seq technique and found that MCAM expression was markedly upregulated in RAGE$^{-/-}$ fibroblasts compared to its expression in WT fibroblasts (Supplementary Fig. 3, available at: https://www.dropbox.com/sh/pl31smto8gq5v8v/AAAFle3bURFnT8-eRhh4V6FJa?dl=0). Its expression was further enhanced by stimulation of the cells with S100A11. From these insights, we consider that MCAM may act as another S100A11 receptor like RAGE in a compensatory manner. Further studies are required to clarify the predicted compensation mechanism(s) in fibroblasts.

Considering the role of fibroblasts in PDAC, we should not disregard the presence of the origin of fibroblasts, mesenchymal stem cells (MSCs), in the PDAC stroma[36]. Recently, we reported that the expression and secretion of amphiregurin (AREG) is significantly enhanced in PDAC cells through MSC interaction in coculture settings. This was also the case in an in vivo condition[37]. These results combined with the results of our previous study showing that there is a feed forward loop formation between secreted S100A11 and EGF family proteins including AREG in cancer cells[9] indicate that MSCs may play a role in S100A11 induction and secretion in PDAC cells at a significant level that in turn activates fibroblast proliferation.

Last, we discuss the usefulness of our identified paracrine pathway as a therapeutic target of PDACs. Through the pathway, targeting mTOR may provide a benefit for suppression of the proliferation of both PDAC cells and PDAC-related fibroblasts. The reason is as follows: multiple signaling cascades triggered by ligands–receptors other than S100A11–RAGE are linked to the activation of mTOR, and multiple downstream molecules including p70 S6 kinase that are associated with tumor progression will be activated constantly by mTOR[38] (i.e., mTOR is a central molecule to tether multiple diverse signals between upstream and downstream). In addition, targeting mTOR is expected to affect not only fibroblasts but also the cancer site. Tommelein et al. reported an unusual role of mTOR in the progression of colorectal cancers (CCs) in patients who received neoadjuvant radiotherapy[39]. They revealed that abundant CAFs in CC microenvironments produce insulin-like growth factor (IGF1) at a significant level in response to radiation stress, by which cancer cells receive IGF1 by their own cell surface IGFR, resulting in the acquisition of a highly aggressive phenotype through mTOR. Hepatocyte growth factor (HGF) from CAFs in PDACs shows similar activity[40]. Surprisingly, mTOR inhibition also had a marked preventive effect on fibrosis in an experimental animal model[41]. Taken together, the results indicate that inhibition of mTOR may become a potential treatment for difficult PDACs.

In conclusion, our results support the notion that S100A11 secretion induced by PDAC cells initiates a paracrine activation loop through the RAGE–mTOR–p70 S6 kinase-mediated proliferation pathway in adjacent fibroblasts. Our results support the idea that targeting the paracrine or paracrine-mediated pathway, especially in mTOR, may be an effective approach for improving the therapeutic outcome in difficult PDACs.

ACKNOWLEDGMENTS: We thank the central research center for Kawasaki Medical School for technical support. This work was supported by the Foundation for Promotion of Cancer Research (M. Sakaguchi) and in part by grants from the JSPS KAKENHI Grant (No. 17H03577) (M. Sakaguchi), JSPS KAKENHI Grant (No. 15K10201) (A. Yamauchi), and Takeda Science Foundation (M. Sakaguchi). The authors declare no conflicts of interest.

REFERENCES

1. Shan T, Chen S, Chen X, Lin WR, Li W, Ma J, Wu T, Cui X, Ji H, Li Y, Kang Y. Cancer-associated fibroblasts enhance pancreatic cancer cell invasion by remodeling the metabolic conversion mechanism. Oncol Rep. 2017;37(4):1971–9.
2. von Ahrens D, Bhagat TD, Nagrath D, Maitra A, Verma A. The role of stromal cancer-associated fibroblasts in pancreatic cancer. J Hematol Oncol. 2017;10(1):76.
3. Zhang A, Qian Y, Ye Z, Chen H, Xie H, Zhou L, Shen Y, Zheng S. Cancer-associated fibroblasts promote M2 polarization of macrophages in pancreatic ductal adenocarcinoma. Cancer Med. 2017;6(2):463–70.
4. Bolm L, Cigolla S, Wittel UA, Hopt UT, Keck T, Rades D, Bronsert P, Wellner UF. The role of fibroblasts in pancreatic cancer: Extracellular matrix versus paracrine factors. Transl Oncol. 2017;10(4):578–88.

5. Hwang RF, Moore T, Arumugam T, Ramachandran V, Amos KD, Rivera A, Ji B, Evans DB, Logsdon CD. Cancer-associated stromal fibroblasts promote pancreatic tumor progression. Cancer Res. 2008;68(3):918–26.
6. Xing F, Saidou J, Watabe K. Cancer associated fibroblasts (CAFs) in tumor microenvironment. Front Biosci. (Landmark Ed) 2010;15:166–79.
7. Sakaguchi M, Huh NH. S100A11, a dual growth regulator of epidermal keratinocytes. Amino Acids 2011;41(4): 797–807.
8. Xiao MB, Jiang F, Ni WK, Chen BY, Lu CH, Li XY, Ni RZ. High expression of S100A11 in pancreatic adenocarcinoma is an unfavorable prognostic marker. Med Oncol. 2012;29(3):1886–91.
9. Sakaguchi M, Sonegawa H, Murata H, Kitazoe M, Futami J, Kataoka K, Yamada H, Huh NH. S100A11, an dual mediator for growth regulation of human keratinocytes. Mol Biol Cell 2008;19(1):78–85.
10. Saho S, Satoh H, Kondo E, Inoue Y, Yamauchi A, Murata H, Kinoshita R, Yamamoto K, Futami J, Putranto EW, Ruma IMW, Sumardika IW, Youyi C, Suzawa K, Yamamoto H, Soh J, Tomida S, Sakaguchi Y, Saito K, Iioka H, Huh N, Toyooka S, Sakaguchi M. Active secretion of dimerized S100A11 induced by the peroxisome in mesothelioma cells. Cancer Microenviron. 2016;9(2–3):93–105.
11. Sato H, Sakaguchi M, Yamamoto H, Tomida S, Aoe K, Shien K, Yoshioka T, Namba K, Torigoe H, Soh J, Tsukuda K, Tao H, Okabe K, Miyoshi S, Pass HI, Toyooka S. Therapeutic potential of targeting S100A11 in malignant pleural mesothelioma. Oncogenesis 2018;7(1):11.
12. Sakaguchi M, Murata H, Yamamoto K, Ono T, Sakaguchi Y, Motoyama A, Hibino T, Kataoka K, Huh NH. TIRAP, an adaptor protein for TLR2/4, transduces a signal from RAGE phosphorylated upon ligand binding. PLoS One 2011;6(8):e23132.
13. Futami J, Atago Y, Azuma A, Putranto EW, Kinoshita R, Murata H, Sakaguchi M. An efficient method for the preparation of preferentially heterodimerized recombinant S100A8/A9 coexpressed in Escherichia coli. Biochem Biophys Rep. 2016;6:94–100.
14. Sakaguchi M, Watanabe M, Kinoshita R, Kaku H, Ueki H, Futami J, Murata H, Inoue Y, Li SA, Huang P, Putranto EW, Ruma IM, Nasu Y, Kumon H, Huh NH. Dramatic increase in expression of a transgene by insertion of promoters downstream of the cargo gene. Mol Biotechnol. 2014;56(7):621–30.
15. Kinoshita R, Sato H, Yamauchi A, Takahashi Y, Inoue Y, Sumardika IW, Chen Y, Tomonobu N, Araki K, Shien K, Tomida S, Torigoe H, Namba K, Kurihara E, Ogoshi Y, Murata H, Yamamoto KI, Futami J, Putranto EW, Ruma IMW, Yamamoto H, Soh J, Hibino T, Nishibori M, Kondo E, Toyooka S, Sakaguchi M. Newly developed anti-S100A8/A9 monoclonal antibody efficiently prevents lung tropic cancer metastasis. Int J Cancer 2018. [Epub ahead of print]
16. Kinoshita R, Sato H, Yamauchi A, Takahashi Y, Inoue Y, Sumardika IW, Chen Y, Tomonobu N, Araki K, Shien K, Tomida S, Torigoe H, Namba K, Kurihara E, Ogoshi Y, Murata H, Yamamoto KI, Futami J, Putranto EW, Winarsa Ruma IM, Yamamoto H, Soh J, Hibino T, Nishibori M, Kondo E, Toyooka S, Sakaguchi M. exSSSRs (extracellular S100 Soil Sensor Receptors)-Fc fusion proteins work as prominent decoys to S100A8/A9-induced lung tropic cancer metastasis. Int J Cancer 2018. [Epub ahead of print]
17. Sakaguchi M, Miyazaki M, Inoue Y, Tsuji T, Kouchi H, Tanaka T, Yamada H, Namba M. Relationship between contact inhibition and intranuclear S100C of normal human fibroblasts. J Cell Biol. 2000;149(6):1193–206.
18. Sakaguchi M, Miyazaki M, Sonegawa H, Kashiwagi M, Ohba M, Kuroki T, Namba M, Huh NH. PKCalpha mediates TGFbeta-induced growth inhibition of human keratinocytes via phosphorylation of S100C/A11. J Cell Biol. 2004;164(7):979–84.
19. Sakaguchi M, Miyazaki M, Takaishi M, Sakaguchi Y, Makino E, Kataoka N, Yamada H, Namba M, Huh NH. S100C/A11 is a key mediator of Ca(2+)-induced growth inhibition of human epidermal keratinocytes. J Cell Biol. 2003;163(4):825–35.
20. Chen KT, Kim PD, Jones KA, Devarajan K, Patel BB, Hoffman JP, Ehya H, Huang M, Watson JC, Tokar JL, Yeung AT. Potential prognostic biomarkers of pancreatic cancer. Pancreas 2014;43(1):22–7.
21. Ohuchida K, Mizumoto K, Yu J, Yamaguchi H, Konomi H, Nagai E, Yamaguchi K, Tsuneyoshi M, Tanaka M. S100A6 is increased in a stepwise manner during pancreatic carcinogenesis: Clinical value of expression analysis in 98 pancreatic juice samples. Cancer Epidemiol Biomarkers Prev. 2007;16(4):649–54.
22. Shen J, Person MD, Zhu J, Abbruzzese JL, Li D. Protein expression profiles in pancreatic adenocarcinoma compared with normal pancreatic tissue and tissue affected by pancreatitis as detected by two-dimensional gel electrophoresis and mass spectrometry. Cancer Res. 2004;64(24): 9018–26.
23. Hiratsuka S, Ishibashi S, Tomita T, Watanabe A, Akashi-Takamura S, Murakami M, Kijima H, Miyake K, Aburatani H, Maru Y. Primary tumours modulate innate immune signalling to create pre-metastatic vascular hyperpermeability foci. Nat Commun. 2013;4:1853.
24. Sinha P, Okoro C, Foell D, Freeze HH, Ostrand-Rosenberg S, Srikrishna G. Proinflammatory S100 proteins regulate the accumulation of myeloid-derived suppressor cells. J Immunol. 2008;181(7):4666–75.
25. Zhao F, Hoechst B, Duffy A, Gamrekelashvili J, Fioravanti S, Manns MP, Greten TF, Korangy F. S100A9 a new marker for monocytic human myeloid-derived suppressor cells. Immunology 2012;136(2):176–83.
26. Sakaguchi M, Kinoshita R, Putranto EW, Ruma IMW, Sumardika IW, Youyi C, Tomonobu N, Yamamoto K, Murata H. Signal diversity of receptor for advanced glycation end products. Acta Med Okayama 2017;71(6):459–65.
27. Laird MH, Rhee SH, Perkins DJ, Medvedev AE, Piao W, Fenton MJ, Vogel SN. TLR4/MyD88/PI3K interactions regulate TLR4 signaling. J Leukoc Biol. 2009;85(6):966–77.
28. Ma C, Spies NP, Gong T, Jones CX, Chu WM. Involvement of DNA-PKcs in the type I IFN response to CpG-ODNs in conventional dendritic cells in TLR9-dependent or -independent manners. PLoS One 2015;10(3):e0121371.
29. Chang J, Burkett PR, Borges CM, Kuchroo VK, Turka LA, Chang CH. MyD88 is essential to sustain mTOR activation necessary to promote T helper 17 cell proliferation by linking IL-1 and IL-23 signaling. Proc Natl Acad Sci USA 2013;110(6):2270–5.
30. Hudson BI, Kalea AZ, Del Mar Arriero M, Harja E, Boulanger E, D'Agati V, Schmidt AM. Interaction of the RAGE cytoplasmic domain with diaphanous-1 is required for ligand-stimulated cellular migration through activation of Rac1 and Cdc42. J Biol Chem. 2008;283(49):34457–68.

31. Yamamoto K, Murata H, Putranto EW, Kataoka K, Motoyama A, Hibino T, Inoue Y, Sakaguchi M, Huh NH. DOCK7 is a critical regulator of the RAGE-Cdc42 signaling axis that induces formation of dendritic pseudopodia in human cancer cells. Oncol Rep. 2013;29(3):1073–9.
32. Hibino T, Sakaguchi M, Miyamoto S, Yamamoto M, Motoyama A, Hosoi J, Shimokata T, Ito T, Tsuboi R, Huh NH. S100A9 is a novel ligand of EMMPRIN that promotes melanoma metastasis. Cancer Res. 2013;73(1):172–83.
33. Ruma IM, Putranto EW, Kondo E, Murata H, Watanabe M, Huang P, Kinoshita R, Futami J, Inoue Y, Yamauchi A, Sumardika IW, Youyi C, Yamamoto K, Nasu Y, Nishibori M, Hibino T, Sakaguchi M. MCAM, as a novel receptor for S100A8/A9, mediates progression of malignant melanoma through prominent activation of NF- B and ROS formation upon ligand binding. Clin Exp Metastasis 2016;33(6):609–27.
34. Ruma IMW, Kinoshita R, Tomonobu N, Inoue Y, Kondo E, Yamauchi A, Sato H, Sumardika IW, Chen Y, Yamamoto KI, Murata H, Toyooka S, Nishibori M, Sakaguchi M. Embigin promotes prostate cancer progression by S100A4-dependent and -independent mechanisms. Cancers (Basel) 2018;10(7).
35. Sakaguchi M, Yamamoto M, Miyai M, Maeda T, Hiruma J, Murata H, Kinoshita R, Winarsa Ruma IM, Putranto EW, Inoue Y, Morizane S, Huh NH, Tsuboi R, Hibino T. Identification of an S100A8 receptor neuroplastin- and its heterodimer formation with EMMPRIN. J Invest Dermatol. 2016;136(11):2240–50.
36. Kabashima-Niibe A, Higuchi H, Takaishi H, Masugi Y, Matsuzaki Y, Mabuchi Y, Funakoshi S, Adachi M, Hamamoto Y, Kawachi S, Aiura K, Kitagawa Y, Sakamoto M, Hibi T. Mesenchymal stem cells regulate epithelial-mesenchymal transition and tumor progression of pancreatic cancer cells. Cancer Sci. 2013;104(2):157–64.
37. Saito K, Sakaguchi M, Maruyama S, Iioka H, Putranto EW, Sumardika IW, Tomonobu N, Kawasaki T, Homma K, Kondo E. Stromal mesenchymal stem cells facilitate pancreatic cancer progression by regulating specific secretory molecules through mutual cellular interaction. J Cancer 2018;9(16):2916–29.
38. Conciatori F, Bazzichetto C, Falcone I, Pilotto S, Bria E, Cognetti F, Milella M, Ciuffreda L. Role of mTOR signaling in tumor microenvironment: An overview. Int J Mol Sci. 2018;19(8).
39. Tommelein J, De Vlieghere E, Verset L, Melsens E, Leenders J, Descamps B, Debucquoy A, Vanhove C, Pauwels P, Gespach CP, Vral A, De Boeck A, Haustermans K, de Tullio P, Ceelen W, Demetter P, Boterberg T, Bracke M, De Wever O. Radiotherapy-activated cancer-associated fibroblasts promote tumor progression through paracrine IGF1R activation. Cancer Res. 2018;78(3):659–70.
40. Ohuchida K, Mizumoto K, Murakami M, Qian LW, Sato N, Nagai E, Matsumoto K, Nakamura T, Tanaka M. Radiation to stromal fibroblasts increases invasiveness of pancreatic cancer cells through tumor-stromal interactions. Cancer Res. 2004;64(9):3215–22.
41. Yue H, Zhao Y, Wang H, Ma F, Liu F, Shen S, Hou Y, Dou H. Anti-fibrosis effect for Hirsutella sinensis mycelium based on inhibition of mTOR p70S6K phosphorylation. Innate Immun. 2017;23(7):615–24.